

## Structure and Absolute Configuration of Karlotoxin-2, an Ichthyotoxin from the Marine Dinoflagellate *Karlodinium veneficum*

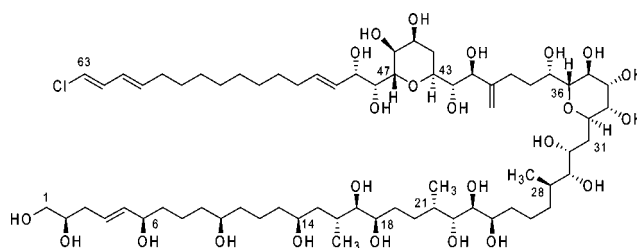
Jiangnan Peng,<sup>†,‡</sup> Allen R. Place,<sup>\*,‡</sup> Wesley Yoshida,<sup>§</sup> Clemens Anklin,<sup>||</sup> and Mark T. Hamann<sup>\*,†,‡,¶</sup>

Department of Pharmacognosy and National Center for Natural Products Research, Department of Pharmacology, School of Pharmacy, and Department of Chemistry & Biochemistry, University of Mississippi, University, Mississippi 38677, Center of Marine Biotechnology, University of Maryland Biotechnology Institute, Suite 236 Columbus Center, Baltimore, Maryland 21202, Department of Chemistry, University of Hawaii at Manoa, Honolulu, Hawaii 96822, and Bruker BioSpin, 15 Fortune Drive, Billerica, Massachusetts 01821

Received October 28, 2009; E-mail: place@umbi.umd.edu.; mthamann@olemiss.edu

An increase in the frequency of ocean disease events over the past two decades with significant implications for marine life has contributed to rising awareness of environmental and human health issues in marine/estuarine environments and the need for rigorous scientific approaches to address them.<sup>1</sup> On July 30, 1996 a large mortality of ~15 000 1–1.25 lb hybrid striped bass occurred during a dinoflagellate bloom at Hyrock Fish Farm in Maryland. After that, many massive fish-kill events have been attributed to this organism. These events were unusual because human health effects among individuals exposed to the presumably contaminated waters were reported, leading to descriptions of a new toxic exposure syndrome characterized by unique skin lesions, respiratory problems, and neurological complications, primarily including short-term memory loss.<sup>2</sup> These have resulted in substantial economic losses in the local seafood and tourism industries. These events have in the past been attributed to the dinoflagellate *Pfiesteria piscicida*,<sup>3</sup> but controversial results have been reported about *Pfiesteria* toxins.<sup>4</sup> Several structural classes have been proposed for the *Pfiesteria* toxin, and a highly labile copper-containing organometallic complex has been proposed as the putative toxin in a recent report.<sup>5</sup> A definitive link between *P. piscicida* and these events has yet to be conclusively determined after 13 years and countless fish kills.

In an attempt to determine the cause of repeated “*Pfiesteria*-associated” fish kills in Maryland, a co-occurring dinoflagellate, *Karlodinium veneficum*, was identified and subsequently shown to produce a unique suite of water-soluble toxins called karlotoxins (KmTx’s) with hemolytic, cytotoxic, and ichthyotoxic properties.<sup>6</sup> To date these toxins have been detected in situ and in clonal isolates collected from estuarine waters from Maryland, North and South Carolina, Georgia, Florida, and Mississippi as well as isolates from New Zealand, Norway, and the English Channel. In addition, these same toxins were isolated directly from water samples collected during fish kills in a South Carolina brackish water pond,<sup>7</sup> at fish kills in a tributary of the Chesapeake Bay, and from the Swan River in Perth, Australia.<sup>8</sup> In all cases, high densities of *K. veneficum* were found, regardless of the presence of *P. piscicida*. The principal toxin isolated both from cultured cells and directly from water samples collected during the fish kills, KmTx2, was similar but not identical to the karlotoxin isolated from cultures and fish kills in Maryland (KmTx1).<sup>9</sup>



Karlotoxin 2 (KmTx2) (1)

KmTx2 was obtained from a clonal culture of *K. veneficum* (CCMP 2064) collected from a fish kill in Georgia. The molecular formula  $C_{67}H_{121}ClO_{24}$  was deduced from detailed analysis of NMR data and the high-resolution ESI–TOF mass spectrometric molecular ion series  $m/z$  1367.7844 ( $[M + Na]^+$ , calcd 1367.7829) and 695.3883 ( $[M + 2Na]^{2+}$ , calcd 695.3866), with careful comparison with simulated isotope pattern data for this formula. Partial structures were assigned on the basis of the preliminary NMR spectral data obtained from a limited quantity of unenriched material (<1 mg), which clearly revealed a polyketide.  $^{13}C$ -enriched KmTx2 (1.3 mg) was prepared from 40 L of culture with  $NaH^{13}CO_3$  (50 mg/L). From this uniformly  $^{13}C$ -enriched sample (10%  $^{13}C$ ), high-quality  $^{13}C$ , DEPT, HMQC, HMBC, and 2D INADEQUATE NMR spectra were obtained using a 600 MHz NMR instrument equipped with a dual CryoProbe. The carbon backbone connections of C1–C22, C23–C33, C34–C39, C40–C53, and C58–C63 were established from the 2D INADEQUATE spectrum and verified by COSY, TOCSY, HSQC and HMBC spectra. A weak INADEQUATE correlation between C30 and C31 was validated by the COSY correlations between H30 at  $\delta$  3.91 and H31 at  $\delta$  1.84 and 1.70. The connection of C22 and C23 was confirmed by the HMBC correlations of H23 to C22 and C21 and of H22 to C23 and C24 as well as by the COSY correlation between H22 at  $\delta$  3.69 and H23 at  $\delta$  3.33. The connection of C39 and C40 was deduced from the correlations of H67 at  $\delta$  5.08 and 5.03 and H41 at  $\delta$  4.23 to C39 at  $\delta$  27.56 and of H39 at  $\delta$  2.45 and 2.15 and H38 at  $\delta$  1.70 to C40 at  $\delta$  151.40. Although the resonances of H33 and H34 overlap at  $\delta$  3.73 and the resonances of C33 and C34 at  $\delta$  73.17 and 73.18 are too close to be distinguished in the 2D NMR spectra, the connection of C33 and C34 was established by the HMBC correlation between  $\delta$  3.73 and  $\delta$  73.17/73.18, which can only be reasonably explained as the correlation between H33 and C34 and that between H34 and C33. The  $(CH_2)_4$  moiety linking C53 and C58 was deduced from the DEPT and HMQC spectra, the molecular formula, and the  $^{13}C$  shift values. The ether bridge between C43 and C47 and that between C32 and C36 were determined by the

<sup>†</sup> Department of Pharmacognosy and National Center for Natural Products Research, University of Mississippi.

<sup>‡</sup> University of Maryland Biotechnology Institute.

<sup>§</sup> University of Hawaii at Manoa.

<sup>||</sup> Bruker BioSpin.

<sup>†</sup> Department of Pharmacology, School of Pharmacy, University of Mississippi.

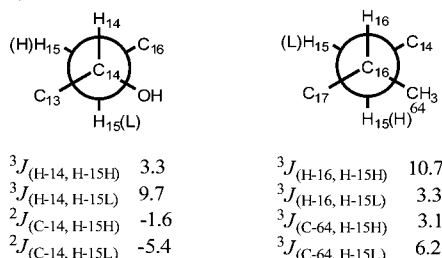
<sup>¶</sup> Department of Chemistry & Biochemistry, University of Mississippi.

<sup>v</sup> Current address: Department of Pharmacology, University of Texas Health Science Center at San Antonio, 7703 Floyd Curl Drive, San Antonio, TX 78229.

HMBC correlations of H47 at  $\delta$  3.74 to C43 at  $\delta$  70.40 and H36 at  $\delta$  3.40 to C32 at  $\delta$  74.72, respectively.<sup>10</sup>

The relative configurations of the two pyran rings were determined using chemical shifts, coupling constants, and NOE interactions. The relative configurations of substructures C14–C18, C21–C24, C28–C37, and C41–C49 were established using  $J$ -based configuration analysis,<sup>11</sup> while the relative configurations of the isolated chiral centers at C2, C6, and C10 could not be resolved by this technique. This method was reported by Murata et al.<sup>11</sup> for the analysis of the relative configurations of polyhydroxylated acyclic molecules by detailed analysis the  $^3J_{\text{H,H}}$  and  $^2,^3J_{\text{C,H}}$  values, and it has been successfully applied to several examples,<sup>12</sup> including the determination of the relative configuration of amphidinol 3,<sup>13</sup> with which KmTx2 shares significant structural similarities.  $^3J_{\text{H,H}}$  values were determined by 1D TOCSY and homonuclear decoupling experiments and  $^2,^3J_{\text{C,H}}$  values by sensitivity- and gradient-enhanced hetero ( $\omega_1$ ) half-filtered TOCSY (HETLOC)<sup>14</sup> or 2D gradient-selected HSQMBBC.<sup>15</sup> For example, the relative configurations of C14–C16 were determined through the assignment of the two diastereomeric methylene protons of C15 (Figure 1). The anti orientations of H15(H)/H16 and H15(L)/H14 were suggested by the large  $^3J(\text{H15H}, \text{H16})$  and  $^3J(\text{H15L}, \text{H14})$  values, while the gauche orientations of H15(L)/H16 and H15(H)/H14 were provided by the small  $^3J(\text{H15L}, \text{H16})$  and  $^3J(\text{H15H}, \text{H14})$  values. The anti orientation of H15L/C64 and H15H/C14–OH were shown by large  $^3J(\text{H15L}, \text{C64})$  and small  $^2J(\text{H15H}, \text{C14})$  values. These interactions established the relative configurations of C14–C16 as depicted in Figure 1a. The intermediate coupling constants between H18/H17 and H17/H16 suggested two alternative conformations for both C18/C17 and C17/C16. The small  $^3J(\text{H17}, \text{C19})$  and  $^3J(\text{H17}, \text{C64})$  values indicated that both H17/C19 and H17/C64 remained in a gauche orientation. The  $^2J(\text{H17}, \text{C18})$ ,  $^2J(\text{H18}, \text{C17})$ , and  $^2J(\text{H16}, \text{C17})$  values showed an orientation intermediate between gauche and anti. Thus, the configuration of C16–C18 was determined as shown in Figure 1b. The relative configurations of C21–C24, C28–C32, C36–C37, C41–C43, and C47–C49 were elucidated using the same method (see the Supporting Information).

### a. C14–C16



### b. C16–C18

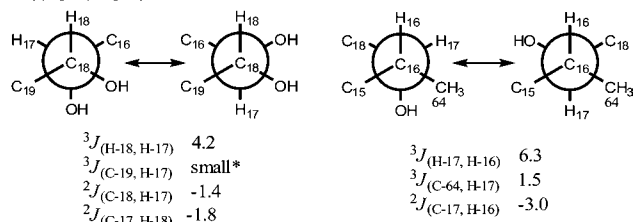


**Figure 1.** Rotamers and coupling constants for C14–C18.

The relative configurations of C37–C41 were correlated using coupling constants and NOE data, as shown in Figure 2. Thus, the configuration of the three subunits C14–C18, C21–C24, and C28–49, were established.

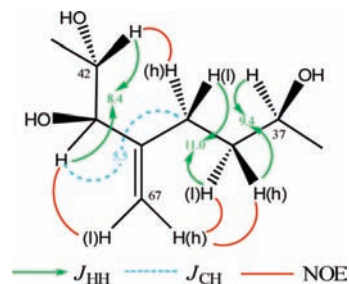


**Figure 2.** Correlation of the relative configurations of C37–C42 using coupling constant and NOE data.

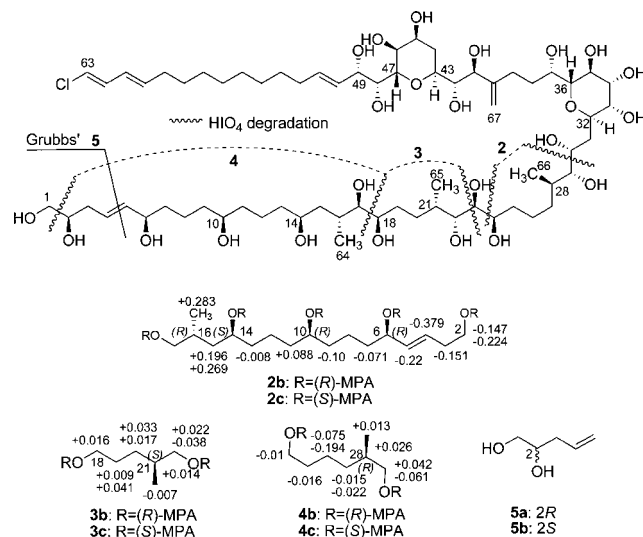


**Figure 3.** Degradation followed by esterification with MPA;  $\Delta\delta^{\text{RS}}$  values are also shown.

To determine the absolute configuration, KmTx2 was first degraded using HIO<sub>4</sub>, then reduced by NaBH<sub>4</sub>, and finally esterified with (*R*)- and (*S*)- $\alpha$ -methoxyphenylacetic acid (MPA). The MPA esters of the degradation products corresponding to C2–C17 (**2b/c**), C18–C22 (**3b/c**), and C24–C29 (**4b/c**) were obtained (Figure 3). The absolute configurations of C6, C10, C14, C21, and C28 were assigned as *R*, *R*, *S*, *S*, *R*, respectively, by comparison of  $\Delta\delta^{\text{RS}}$  between **2b/c**, **3b/c**, and **4b/c** (Figure 3). To verify the absolute configurations of C21 and C28, **3b/c** and **4b/c** were synthesized from dimethyl-(*S*)-2-methylglutarate and (*R*)-3-methylcyclohexanone.<sup>16</sup> The NMR data for the degradation products **3b/c** and **4b/c** matched those of the synthesized **3b/c** and **4b/c**, respectively, which confirmed the configurations of C21 and C28 to be *S* and *R*, respectively. The absolute configurations of C16–C18, C20–C22, and C27–C49 were correlated with C14, C21, and C28, respectively, as shown in Figure 3. To determine the absolute configuration of C2, KmTx2 was degraded through olefin metathesis using Grubbs' catalyst II and excess ethylene to yield pent-4-ene-1,2-diol (**5a** or **5b**). The degradation product exhibited the same retention time in chiral GC–MS with the synthetic *R* enantiomer (**5a**), indicating an *R* configuration for C2 (Figure 3). KmTx2 shares structural similarities to amphidinol 3,<sup>13</sup> while the absolute configuration of the C32–C49 unit is opposite to that in amphidinol 3. The differences in absolute configuration could be due to the limited amount of coupling-constant data available for C28–C32 of KmTx2 or similar challenges with amphidinol 3. Amphidinol 3 shares the same C32–C49 substructure with KmTx2 less a 35-OH group and with the addition of a 31-OH group. The absolute configuration of C32–C49 of amphidinol 3 was determined on the

basis of correlations with C37, whose absolute configuration was deduced from Mosher's esters of the C31–C48 unit of the HIO<sub>4</sub> degradation products.<sup>13</sup> The crowded hydroxyl groups (31, 33, 34, and 37) and the resulting crowded MTPA esters in this degradation subunit (C31–C48) may affect a correct prediction of the absolute configuration of C37 of amphidinol 3 (see the Supporting Information for details).

The purified KmTx2 reproducibly kills fish in a dose-dependent manner. The mortalities in zebrafish and sheepshead minnow juveniles were observed at 0.1–0.5  $\mu\text{g/mL}$ , which is within the concentration range of KmTx2 (0.1–0.8  $\mu\text{g/mL}$ ) in water samples during fish kills.<sup>4</sup> The pathology (sloughing of the epithelium) observed in the laboratory-treated fish gills (Figure 4B) is similar to that observed in fish kills in nature (Figure 4C). Karlotoxins have been shown to be membrane, sterol-specific toxins, which is similar to amphotericin B and amphidinol 3.<sup>17</sup> The sterol binding is greatest for brassicasterol > cholesterol > ergosterol > gymnodinosterol (the dominant sterol found in *K. veneficum*).

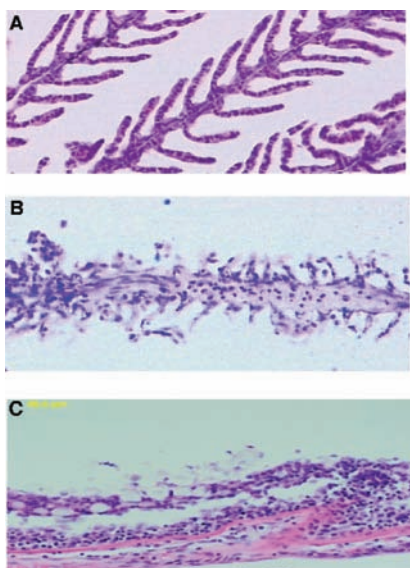


**Figure 4.** Histological sections (5–6  $\mu\text{m}$  thickness) of zebrafish (*Danio rerio*) juveniles stained with hematoxylin and eosin after exposure. (A) Control gill arch. (B) KmTx2 exposure (0.5  $\mu\text{g/mL}$  for 1 h). The loss of intralamellar spacing and secondary lamellar fusion should be noted. (C) Gut epithelia of a striped killifish (*Fundulus majalis*) exposed in situ to karlotoxin ( $\sim 0.2 \mu\text{g/mL}$ ) during a fish-kill event.

*K. veneficum*, formerly *Gyrodinium galatheanum* or *Gymnodinium veneficum*, is distributed worldwide<sup>18</sup> and has been reported to produce toxins since it was first isolated at the Plymouth Marine Laboratory in the United Kingdom by Mary Parke during the 1950s.<sup>19</sup> However, the complete structure of this algal toxin class was not revealed until this report. Karlotoxins are intracellular compounds, and greater than 90% of karlotoxins are cell-associated.

However, they are easily released by shear forces like centrifugation, filtration or passage across gill rakers in feeding menhaden.

**Acknowledgment.** We thank Prof. Michio Murata for pre-viewing this manuscript. This research was supported by NIAID, CDC, the NOAA Coastal Ocean Program, and the Maryland Department of Health and Mental Hygiene. This is contribution no. 10-202 from the UMBI Center of Marine Biotechnology and contribution no. 326 from the Ecology and Oceanography of Harmful Algal Blooms (ECOHAB) Program.

**Supporting Information Available:** Detailed experimental procedures, configuration analysis, biological activity data, and NMR data assignment and spectra for KmTx2. This material is available free of charge via the Internet at <http://pubs.acs.org>.

## References

- (1) Harvell, C. D.; Kim, K.; Burkholder, J. M.; Colwell, R. R.; Epstein, P. R.; Grimes, D. J.; Hofmann, E. E.; Lipp, E. K.; Osterhaus, A. D. M. E.; Overstreet, R. M.; Porter, J. W.; Smith, G. W.; Vasta, G. R. *Science* **1999**, *285*, 1505.
- (2) Grattan, L. M.; Oldach, D.; Perl, T. M.; Lowitt, M. H.; Matuszak, D. L.; Dickson, C.; Parrott, C.; Shoemaker, R. C.; Kauffman, C. L.; Wasserman, M. P.; Hebel, J. R.; Charache, P.; Morris, J. G., Jr. *Lancet* **1998**, *352*, 532.
- (3) Burkholder, J. M.; Glasgow, H. B. *Arch. Protistenkd.* **1995**, *145*, 177.
- (4) Place, A. R.; Saito, K.; Deeds, J. R.; Robledo, J. A. F.; Vasta, G. R. In *Seafood and Freshwater Toxins*, 2nd ed.; Botana, L. M., Ed.; CRC Press: Boca Raton, FL, 2008; pp 717–751.
- (5) Moeller, P. D. R.; Beauchesne, K. R.; Huncik, K. M.; Davis, W. C.; Christopher, S. J.; Riggs-Gelasco, P.; Gelasco, A. K. *Environ. Sci. Technol.* **2007**, *41*, 1166.
- (6) Deeds, J. R.; Terlizzi, D. E.; Adolf, J. E.; Stoecker, D. K.; Place, A. R. *Harmful Algae* **2002**, *1*, 169.
- (7) Kempton, J. W.; Lewitus, A. J.; Deeds, J. R.; Law, J. M.; Place, A. R. *Harmful Algae* **2002**, *1*, 233.
- (8) Goshorn, D.; Deeds, J.; Tango, P.; Poukish, C.; Place, A. R.; McGinty, M.; Butler, W.; Luckett, C.; Magnien, R. In *Harmful Algae 2002: Proceedings of the 10th International Conference on Harmful Algae*; Steidinger, K. A., Landsberg, J. H., Tomas, C. R., Vargo, G. A., Eds.; Fish and Wildlife Conservation Commission, Florida Institute of Oceanography, and Intergovernmental Oceanographic Commission of UNESCO: 2004; pp 361–363.
- (9) Van Wagoner, R. M.; Deeds, J. R.; Satake, M.; Ribeiro, A. A.; Place, A. R.; Wright, J. L. C. *Tetrahedron Lett.* **2008**, *49*, 6457.
- (10) Peng, J.; Hill, R.; Place, A. R.; Anklin, C.; Hamann, M. T. Presented at the 233rd ACS National Meeting, Chicago, IL, March 25–29, 2007; Paper AGFD 30.
- (11) (a) Matsumori, N.; Kaneno, D.; Murata, M.; Nakamura, H.; Tachibana, K. *J. Org. Chem.* **1999**, *64*, 866. (b) Matsumori, N.; Nonomura, T.; Sasaki, M.; Murata, M.; Tachibana, K.; Satake, M.; Yasumoto, T. *Tetrahedron Lett.* **1996**, *37*, 1269.
- (12) (a) Luesch, H.; Yoshida, W. Y.; Moore, R. E.; Paul, V. J.; Corbett, T. H. *J. Am. Chem. Soc.* **2001**, *123*, 5418. (b) Wu, M.; Okino, T.; Nogle, L. M.; Marquez, B. L.; Williamson, R. T.; Sitachitta, N.; Berman, F. W.; Murray, T. F.; McGough, K.; Jacobs, R.; Colsen, K.; Asano, T.; Yokokawa, F.; Shioiri, T.; Gerwick, W. *J. Am. Chem. Soc.* **2000**, *122*, 12041.
- (13) (a) Murata, M.; Matsuoka, S.; Matsumori, N. K.; Tachibana, K. *J. Am. Chem. Soc.* **1999**, *121*, 870. (b) Oishi, T.; Kanemoto, M.; Swasono, R.; Matsumori, N.; Murata, M. *Org. Lett.* **2008**, *10*, 5203.
- (14) Uhrin, D.; Batta, G.; Hruby, V. J.; Barlow, P. N.; Kövér, K. E. *J. Magn. Reson.* **1998**, *130*, 155.
- (15) Williamson, R. T.; Márquez, B. L.; Gerwick, W. H.; Kövér, K. E. *Magn. Reson. Chem.* **2000**, *38*, 265.
- (16) Overberger, C. G.; Kaye, H. *J. Am. Chem. Soc.* **1967**, *89*, 5640.
- (17) Houdai, T.; Matsumori, N.; Murata, M. *Org. Lett.* **2008**, *10*, 4191.
- (18) Bachvaroff, T.; Adolf, J. E.; Place, A. R. *J. Phycol.* **2009**, *45*, 137.
- (19) Abbott, B. C.; Ballantine, D. *J. Mar. Biol. Assoc. U.K.* **1957**, *36*, 169.

JA9091853